91.25.-r

Loginov A.A.*, Samoilenko Yu.I.**, Tkachenko V.A.*
*Space Plasma Department,
Space Research Institute NASU & NSAU, Prospect Acad. Glushkova, 40, 03020 Kiev, Ukraine
**Nonlinear Analysis Department, Mathematics Institute NASU,
Str. Tereshchenkovskaya, 3, 01601, Kiev, Ukraine

Magnetic Field Generation by Conductive Fluid Shear Flow

Contents

Abstract

Mathematical models of kinetic laminary hydromagnetic dynamo both for the plane Couette flow and differentially rotating spherical liquid core of the Earth are considered. Threshold values of the magnetic Reynolds number were estimated, taking into account the non-conductivity of limiting shells. Illustrative maps for magnetic fields and currents are presented. Obtained results support tidal hypothesis for the planetary dynamo energetic driver.

1. Introduction

The present paper is written on a study of the laminary dynamo effect [1] that is evident in rather intense laminary shear flows of a conductive fluid with high electric conduction as a spontaneous event and steady-state magnetic field sustenance. The interest in this phenomenon keeps growing as being associated with studies on the magnetism of planets and other outer space bodies (see, Review Paper [2]). An outstanding researcher of the geomagnetic dynamo theory F. Busse cites in his paper [3] an interesting historical fact that A. Einstein referred the problem of the Earth's magnetic field origin to three cardinal unsolved physical problems. In those times, certain scientists believed that the geomagnetism can be accounted for by some yet unknown physical laws. Nowadays its origin is commonly referred to the dynamo effect in the liquid metal core of a planet. The Earth' s cutaway view is shown in Fig. 1, reproduced courtesy to the paper [2].

The physical mechanism of the hydromagnetic dynamo is based on the Faraday inductance law that is mathematically represented as follows for the moving continuous medium, with the relative magnetic permeability being unity and finite conduction:

$$\frac{\partial \vec{H}}{\partial t} = \mathrm{rot}[\vec{V} \times \vec{H}] + \mu \Delta \vec{H}, \qquad (1)$$

where $\vec{H}$ – the magnetic field strength, $\vec{V}$ – the fluid flow velocity, $\mu = 1/\mu_0\sigma = \mathrm{Re}_m^{-1}$ – the magnetic viscosity (μ_0 – the vacuum magnetic permeability, Re_m – the Reynolds magnetic number).

There are two levels of the dynamo effect mathematical modeling : kinematic and magnetohydrodynamic (MHD). On the kinematic level, the velocity field $\vec{V} = \vec{V}(\vec{r})$, ($\vec{r}$ – the radius vector of a point in space) is considered to be assigned, while $\vec{H}$ is computed from (1) at the condition of impermeability of the boundary S for the current $\mathrm{rot}_n \vec{H}\big|_S = 0$. At the MHD level, the velocity field is brought, in its turn, under dependence on the magnetic field according to the Navier-Stokes

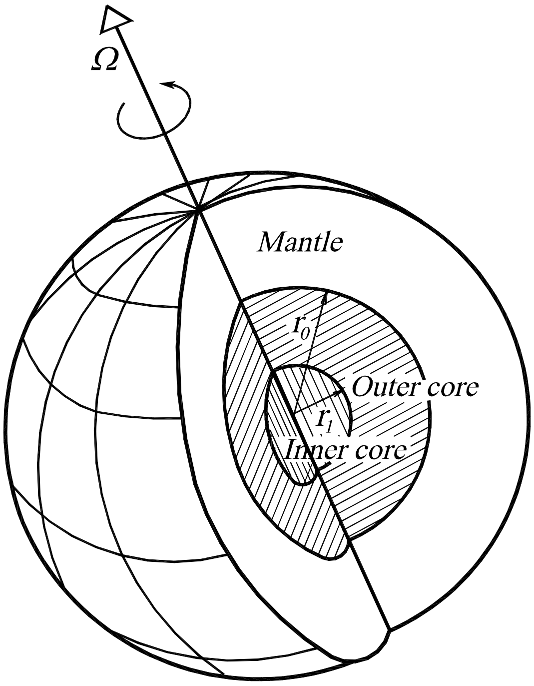

Fig. 1.

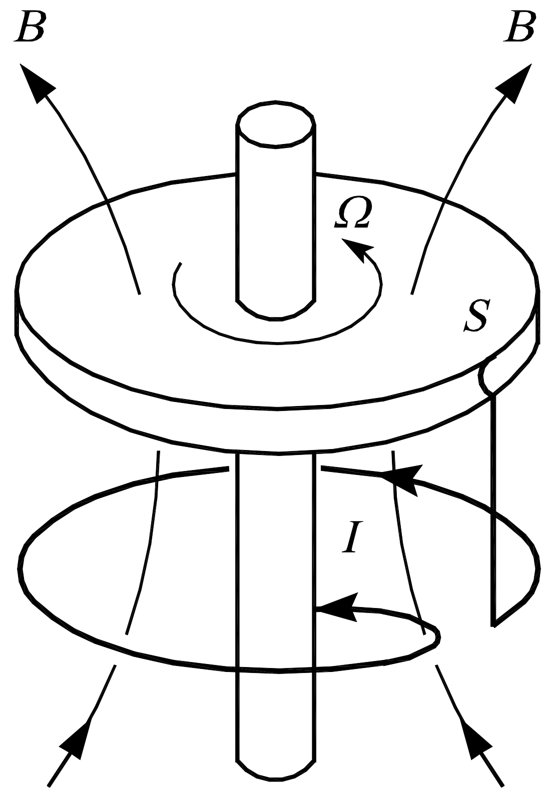

Fig. 2.

equation in consideration of the ponderomotive forces. This equation can be written in the following way in the immobile coordinate system for incompressible viscous fluid with the unity mass density:

$$\frac{\partial \vec{V}}{\partial t} + (\vec{V}\cdot\vec{\nabla})\vec{V} = -\mathrm{grad}\, p - [\vec{H}\times \mathrm{rot}\vec{H}] + \vartheta\Delta\vec{V}, \quad (\mathrm{div}\vec{V}=0). \quad (2)$$

Here p is the hydrodynamic pressure, ϑ – the kinematic viscosity.

In order to study the possibility of the magnetic field-self excitation and determine the threshold value of the Reylnods magnetic number Re_m^* vs. the flow velocity field in the assigned region and boundary conditions, it is just sufficient to employ the kinematic dynamo model which is evidently linear. While considering a mature stage of the dynamo process, it is necessary to resort to the complete non-linear MHD equation set.

The dynamo effect, in itself, is not particularly surprising, being manifest in the model of the disk homopolar Bullard dynamo the schematic of which is shown in Fig. 2, as taken from the paper [1].

This effect becomes less obvious for the case of the hydromagnetic dynamo, since the electric current vector field is not known a priori in the moving liquid conductor as distinct from the dynamo machines with an assigned geometry of the electric current. In the meantime, trying to solve the boundary problem of the hydromagnetic dynamo, even on the kinematic level, brings one up against considerable mathematical difficulties. Attempts of its simplification due to assumptions of the symmetry run into the prohibition imposed by the well-known Cowling theorem [4], which proves the impossibility of axially symmetric dynamo processes. However, the liquid metal Earth's core is practically axially symmetric, which is why the problem of applicability of the dynamo theory to explanation of the geomagnetism had remained unsolved for a long time.

An opinion exists [3] that the first mathematically convincing evidence in favor of the geomagnetic dynamo was postulated in 1958 by Backas [5] and Herzenberg [6] who had employed a convective mechanism of the non-axially symmetric shear flow in a liquid core, although regarding the solar plasma where convective processes are by far more intense than in the Earth's liquid metal core, the MHD nature of solar spots was explained way back in 1919 by Larmore [7]. The ideas of Backas and Herzenberg were further elaborated in the papers [1,3,8,9]. In the subsequent years the concepts of weakly axially symmetric and turbulent dynamo [10,11] were elaborated as well as the concepts of magnetostrophic wave processes [1].

One of the principal points in the theory of planetary magnetism remains the problem of energy drive, causing shear flows in liquid cores. This issue is open to discussion to date. Owing to the extreme inefficiency of thermoconvective processes in condensed media in comparison with processes in the

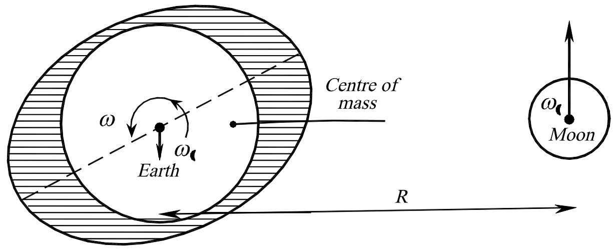

Fig. 3. Origin of the tidal moment. The Moon's attraction potential gradient causes appearance of the tidal bulges on the Earth, particularly in the oceans. The energy dissipation processes causes a delay of the tides. The tidal bulges gravitational potential gradient creates a force that accelerates the Moon orbital movement and a force that slows down rotation of the Earth. The Earth rotates around her axis with the angular speed ω. The Earth and the Moon rotate around the common center of mass with the angular speed ω.

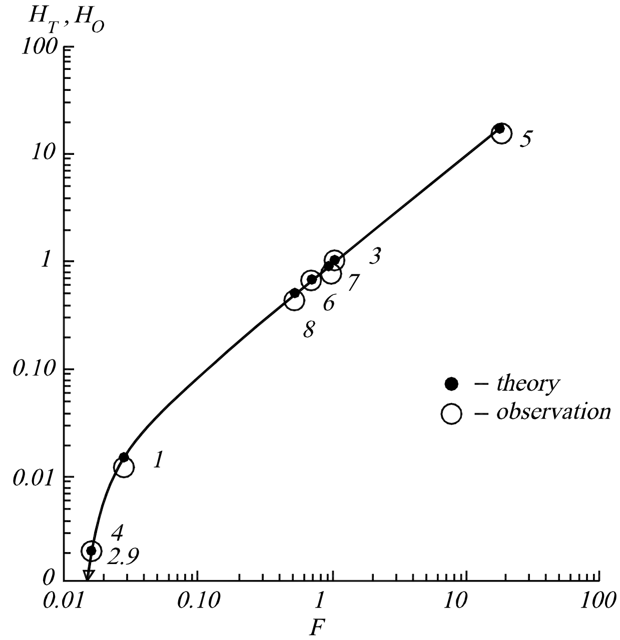

Fig. 4. Magnetic field theoretical value H_τ dependence on F – tidal force. H_0 – observable magnetic field. 1 – Mercury, 2 – Venus, 3 – Earth, 4 – Mars, 5 – Jupiter, 6 – Saturn, 7 – Uranus, 8 – Neptune, 9 – Pluto.

solar and stellar plasmas, many authors suggest to take into consideration the processes of flotation and chemical differentiation of substances in the planet cores.

Despite the fact that the kinetic energy of the daily liquid core rotation is quite enough to sustain the dynamo processes during the entire time of the planet existence [3], conversion of this energy into electromagnetic was considered until recently to be feasible only via the precession mechanism [12]. The other tidal mechanism that causes slowdown of the planet external shell by the gravitational forces from planet's satellites or the Sun, for example, using the Earth-Moon interactions scheme, as given in Fig. 3 (according to [17]), could also be considered as an energy driver of the dynamo process. To achieve this, it must cause such a shear flow in the liquid core that is capable to sustain magnespite the fact that the kinetic energy of the daily liquid core rotation is quite enough to sustain the dynamo processes during the entire time of the planet existence [3], conversion of this energy into electromagnetic was considered until recently to be feasible only via the precession mechanism [12]. The other tidal mechanism that causes slowdown of the planet external shell by the gravitational forces from planet's satellites or the Sun, for example, using the Earth-Moon interactions scheme, as given in Fig.3 (according to [17]), could also be considered as an energy driver of the dynamo process. To achieve this, it must cause such a shear flow in the liquid core that is capable to sustain magnetic field generation.

The tidal mechanism of the dynamo process excitation was not paid much attention to, since it was supposed that the flow it created must have predominantly the toroidal field velocity component, and, moreover, according to Proudman [13] it was nearly solid-state. Even if it were not solid-state, then, as Elsasser asserted in the so-called "toroidal theorem" [14], a purely toroidal velocity field cannot produce a continuously operating dynamo. Nonetheless, Cowling in his book [15] indicates independent numerical experiments by Gubbins, and also by Pekeris, Akkada and Scholer, that quite to the contrary supported the feasibility of sustaining the magnetic field by axially symmetrical flows at the condition that the harmonics of this field are not axially-symmetric themselves. It goes without saying that in such approach to the modeling there appears no contradiction to the Cowling theorem, although questions arise concerning the relevance of the "toroidal theorem".

A recently published paper by Krechetov [15] proves beyond any shade of doubt (Fig. 4) the tidal hypothesis, using the example of all the planets of the solar system that have a noticeable tidal slowdown. The data, contained in this Figure, indicates that all the planets that have rather massive satellites, slowing down their external shells, as well as Mercury that suffers from the tidal slowdown from the Sun, have a considerable magnetic field. The other planets, including Venus (Earth group planets) that have no massive satellites, practically do not have magnetic field.

With the above-said in mind, the authors of the present paper deem it necessary to study in more detail the hydromagnetic dynamo, taking for basis the tidal slowdown hypothesis. It is useful to consider preliminarily a simpler model of the laminary

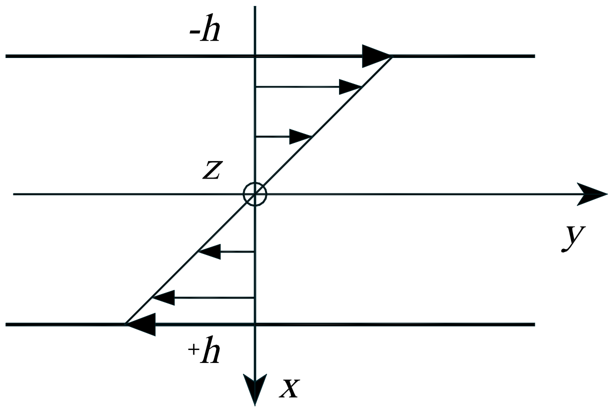

Fig. 5.

kinematic dynamo, excited by the Couette plane shear flow in a conductive liquid.

2. Magnetic field generation by the Couette plane flow of conductive liquid

Let us consider in the Cartesian coordinates $\{\vec{e}_x, \vec{e}_y, \vec{e}_z\}$ the Couette flow of conducting fluid with the velocity profile

$$\vec{V} = -\vec{e}_y \Omega x \qquad (-h \le x \le h, [\Omega] = c^{-1}), \quad (3)$$

that is created by two fluid-driving non-conducting plates, moving in the direction $\vec{e}_y$ and being equidistant on h from the plane $\{y, z\}$, as shown in Fig. 5.

Choosing for convenience the system of units for measuring the length and time in which $h = 1$, $\Omega = 1$, we will write down the equations, determining the field $\vec{H}$ and providing for current non-flowing through the plates in the following form:

$$\begin{aligned} &\frac{\partial \vec{H}}{\partial t} + \mathrm{rot}[x\vec{e}_y \times \vec{H}] = \mu \Delta \vec{H}, \\ &\mathrm{div}\vec{H} = 0, \\ &\mathrm{rot}_x \vec{H}\big|_{x=\pm 1} = 0. \end{aligned} \quad (4)$$

Considering their linearity and translation invariance relative to t, y, z, the solution will be sought as superposition of the Fourier harmonics:

$$\vec{H} = [\vec{e}_y H_y(x) + \vec{e}_z H_z(x)] e^{\mu\gamma t + i(ky + \ell z)}, \quad (5)$$

assigning the polarization such that $H_x(x) \equiv 0$, and thereby providing for the most total field localization in the region occupied by the flow.

Substitution of (5) in (4) comes out with the relationship $kH_y(x) + \ell H_z(x) = 0$ and boundary problem for $H_z(x)$:

$$H_z''(x) = (k^2 + \ell^2 + \gamma - i\mu^{-1} kx) H_z(x), \qquad (-1 < x < 1), \quad (6)$$

$$H_z(\pm 1) = 0. \quad (7)$$

By replacing the variables

$$Z = -\left(\frac{k}{\mu}\right)^{1/3} \times \left\{\mu k [1 + k^{-1}(\ell^2 + \gamma)] - ix\right\} = Z(x), \quad (8)$$

$$H_z(x) = W(Z)\big|_{Z=Z(x)} \quad (9)$$

the equation (6) is transformed into the Airy one:

$$W''(Z) = ZW(Z). \quad (10)$$

In the meantime, the length $[-1, 1]$ of the real straight line x becomes a rectilinear length on the complex plane Z perpendicular to the real axis and connecting complex conjugate points:

$$Z_{(\pm)} = -a^{1/3} e^{\mp i\varphi}, \quad (11)$$

where a and φ are determined by the following relationships:

$$\begin{aligned} &\mathrm{ctg}\,\varphi = \mu k [1 + k^{-2}(\ell^2 + \gamma)], \\ &a = k^2 [1 + k^{-2}(\ell^2 + \gamma)](1 + \mathrm{tg}^2\,\varphi)^{3/2}\,\mathrm{ctg}^2\,\varphi. \end{aligned} \quad (12)$$

Appropriately, the boundary conditions (7) for $H_z(x)$ are transformed into such boundary conditions that are assigned at the extremities of the said length of the complex plane Z for $W(Z)$:

$$W(Z_{(\pm)}) = 0. \quad (13)$$

Owing to the proposed substitution of the variables, the solution of the boundary problem of interest can now be expressed in whole transcendental Airy functions $\mathrm{Ai}\,(Z)$ that according to [18] are represented as power series converging all over the plane Z in the following way:

$$\mathrm{Ai}\,(Z) = \mathrm{Ai}\,(0) \left[1 + \sum_{n=1}^{\infty} \frac{Z^{3n}}{\prod\limits_{k=1}^{n}(3k-1) \prod\limits_{\ell=1}^{n}(3\ell)}\right] + \mathrm{Ai}\,'(0) \left[Z + \sum_{n=1}^{\infty} \frac{Z^{3n+1}}{\prod\limits_{k=1}^{n}(3k) \prod\limits_{\ell=1}^{n}(3\ell+1)}\right], \quad (14)$$

where

$$\mathrm{Ai}\,(0) = \left[3^{2/3}\Gamma(2/3)\right]^{-1}, \quad \mathrm{Ai}\,'(0) = \left[3^{1/3}\Gamma(1/3)\right]^{-1}.$$

The following functions determined in terms of $\mathrm{Ai}\,(Z)$

$$W_{\pm}(Z) = \mathrm{Ai}\,\left(Z e^{\pm 2\pi i/3}\right) \quad (15)$$

are two linearly independent solutions of the equation (10), as is the very function $\mathrm{Ai}\,(Z) = W(Z)$, connected with $W_{(+)}$ and $W_{(-)}$ linearly:

$$W(Z) + W_{(+)}(Z) e^{2\pi i/3} + W_{(-)}(Z) e^{-2\pi i/3} = 0. \quad (16)$$

The function

$$w(Z) = u(Z) + iv(Z) = 2\sqrt{\pi}W_{(+)}(Z)e^{i\pi/6}, \quad (17)$$

proposed by Fock [19] for application in the theory of radio frequency wave propagation over curving surface has been studied well and tabulated. For the real values $Z = t$, tables of the functions $u(t)$, $v(t)$, $u'(t)$, $v'(t)$ have been compiled, allowing to employ the identity (16) for obtainment of the Airie function values not only on the real axis, but also on six rays of the complex plane on which

$$\arg Z = \frac{n\pi}{3} \qquad (n = 0, 1, 2, 3, 4, 5).$$

However, these tabulated data are not sufficient to solve the dynamo boundary problem, because it is not known a priori exactly which values of Z will be characteristic numbers. For this reason, in order to determine them one should employ a representation in the form of common power series (14), converging all over the complex plane, as well as the Fock-indicated asymptotics for $u(Z)$ and $v(Z)$, that are true across a rather broad sector $-\pi/3 < \arg < \pi/3$, in which the series converge:

$$\begin{aligned} u(Z) &= Z^{-1/4}\exp\left(2/3Z^{3/2}\right)\times \\ &\quad (1 + a_1Z^{-1} + a_2Z^{-2} + a_3Z^{-3} + \dots), \\ v(Z) &= Z^{-1/4}\exp\left(-2/3Z^{3/2}\right)\times \\ &\quad (1 - a_1Z^{-1} + a_2Z^{-2} - a_3Z^{-3} + \dots), \end{aligned} \quad (18)$$

where $a_1 = \dfrac{5}{72}$, $a_2 = \dfrac{(5\cdot 111)\cdot 7}{(1\cdot 2)\cdot 72^2}$,

$a_3 = \dfrac{(5\cdot 11\cdot 17)\cdot(7\cdot 13)}{(1\cdot 2\cdot 3)\cdot 72^3}$, ...,

$a_n = \dfrac{[5\cdot 11\cdot\dots\cdot(6n-1)]\cdot[7\cdot 13\cdot\dots\cdot(6n-5)]}{n!72^n}$.

By using the Airy functions (15), we can represent the total solution of the equation (10) as:

$$W(Z) = C^{(+)}W_{(+)}(Z) + C^{(-)}W_{(-)}(Z). \quad (19)$$

By substituting (19) in the boundary conditions (13), we will obtain a linear uniform algebraic set of two equations relative to two unknown constants C^{+}, $C^{(-)}$:

$$\begin{aligned} C^{(+)}W_{(+)}(Z_{(+)}) + C^{(-)}W_{(-)}(Z_{(+)}) = 0, \\ C^{(+)}W_{(+)}(Z_{(-)}) + C^{(-)}W_{(-)}(Z_{(-)}) = 0. \end{aligned} \quad (20)$$

The non-trivial solution of this set is known to call for and suffice its determinant to be equal to zero. Accordingly, we shall obtain the following characteristic equation:

$$W_{(+)}(Z_{(+)})W_{(-)}(Z_{(-)}) = W_{(+)}(Z_{(-)})W_{(-)}(Z_{(+)}). \quad (21)$$

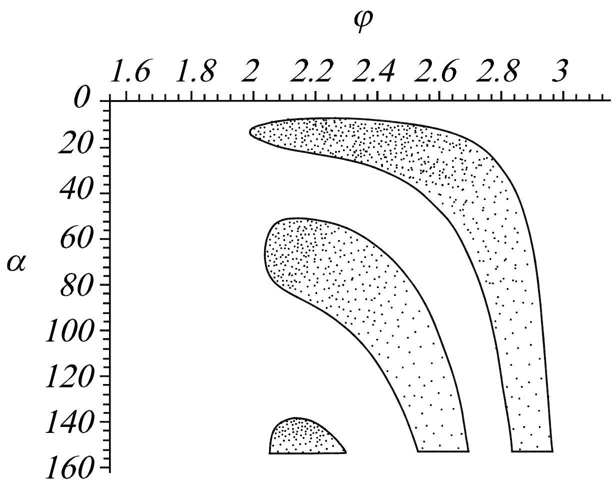

Fig. 6.

Simple computations, using (11), (14), (15), bring this equation to the convenient final form that establishes the inter-connection between a and φ:

$$\sin\varphi + \sum_{n=1}^{\infty}(-1)^n a^n f_n(\varphi) = 0, \quad (22)$$

where

$$f_n(\varphi) = \frac{\prod_{k=1}^{n}(3k-1)}{(3n+1)!}\sin[(3n+1)\varphi] + \sum_{m=1}^{n-1}\frac{\prod_{k=1}^{n-m}(3k-1)\prod_{\ell=1}^{m}(3\ell-2)}{(3m)![3(n-m)+1]!}\sin\{[3(n-2m)+1]\varphi\} - \frac{\prod_{\ell=1}^{n}(3\ell-2)}{(3n)!}\sin[(3n-1)\varphi].$$

The above power series, as follows from the Airie function theory, converges all over the complex plane Z, i.e. at all $a \geq 0$ and any $\varphi(\mathrm{mod}2\pi)$, but the region of existence for solutions of the equation (22) must not, undoubtedly, coincide with the entire plane Z. As analysis indicates, some solutions exist at least in the sector $\pi/2 < \varphi < \pi$.

The calculations were made within the limits $1 < n < N$. Beginning from as low as $N \geq 20$, the further increase of N up to $N = 60$ did not bring out, practically, any differences in the calculation results of the dispersion relationship $a = a(\varphi)$ in the range $0 \leq a \leq 160$. A zone structure of instability becomes apparent in which, as a matter of fact, the dynamo effect comes about. To illustrate the above-said, Fig. 6 shows epures of three zones (they are shaded) coming under the above range of variations of a.

Of principal importance are the threshold value $a_* = a_{\min}$ and the corresponding φ_*. These values determine the highest magnetic viscosity value $\mu =$

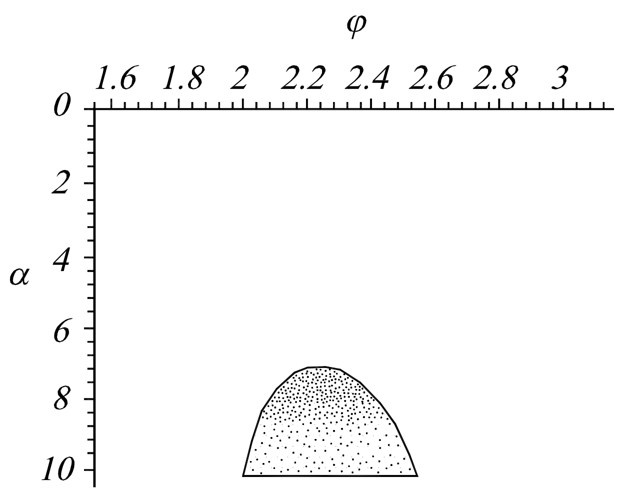

Fig. 7.

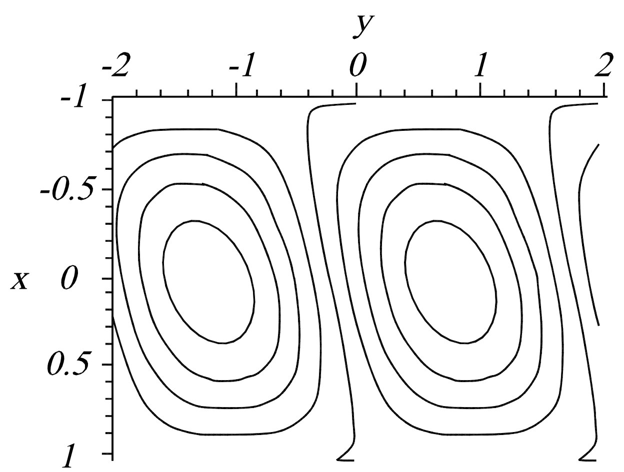

Fig. 8.

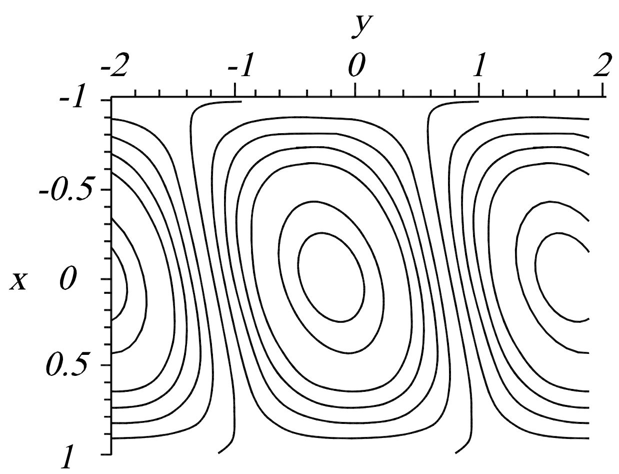

Fig. 9.

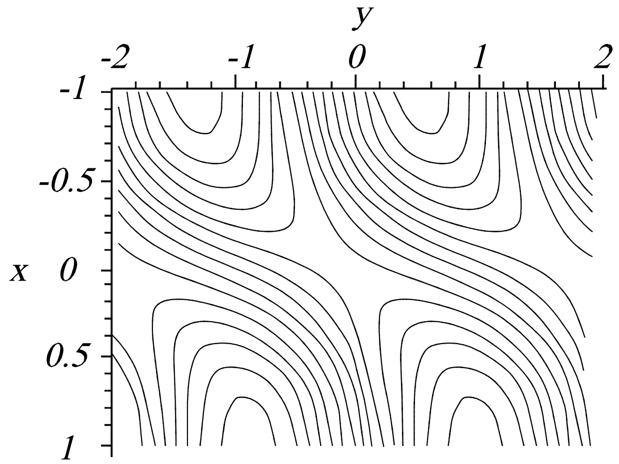

Fig. 10.

$\mu_{\rm cr}$, above which the field generation is not possible, while the least field wavelength, realized at $\mu = \mu_{\rm cr}$, will be $\lambda_{\min} = 2\pi/k_{\rm cr}$, the connection of which with a_* and φ_* is established according to (12). The first zone fragment with a_* and φ_* is shown on the large scale in Fig. 7.

As a result of substitution of the derived dispersion relationship $a = a(\varphi)$ into the formulae, determining $Z_{(\pm)}$, we will obtain such a solution of the equation (10) with the accuracy to the arbitrary multiplier that satisfies the assigned boundary conditions (13) and now appears as:

$$W(Z) = W_{(-)}(Z_{(+)})W_{(+)}(Z) - W_{(+)}(Z_{(+)})W_{(-)}(Z). \quad (23)$$

The explicit expression for $H_z(x)$ is derived from (23) according to the formulae (8) and (9). In the meantime, $H_y(x) = -\ell/kH_z(x)$. The vector current field is determined as a result of performing the operation rot to (5). Bringing out the real part from the derived magnetic field and current expressions comes out with the final real form for the solution of the problem considered.

For the case $\gamma = 0$ and $\ell = 0$ at $a = a_{\rm cr} = 6.970$ and $\varphi_* = 2.247$, corresponding, according to (12), to $k_* = -1.629$ and $\mathrm{Re}^*_m = \mu_*^{-1} = 2.029$, the curves of level in Fig. 8, being within the limits $-0.8 \leq H_z \leq 0.8$, show the results of calculations of the z-component of the magnetic field $\vec{H}$ strength as functions x and y. In much the same way, Fig. 9 and 10 show the distributions of x- and y-components of the current density $\vec{J}$ within the limits -1.5 to $+1.5$.

The above illustrations draw the reader's attention to the following two peculiarities of the constructed epures:

- slanting of the generated field cells and currents toward the shear flow and S-shaping of the zero level curves;

- reversion to zero of the normal to the non-conducting boundaries of the component Jx of the current field in accordance with the assigned boundary conditions.

In a more general case, when $\ell \neq 0$, the dispersion relationship for each field generation zone must be depicted as a family of surfaces, parametrized by the increment γ over the plane of the wave numbers k and ℓ $\mu^{-1} = \mathrm{Re}_m = R^\sigma(k, \ell; \gamma)$, where σ – the number of the zone ($\sigma = 1, 2, 3, \dots$). The minimum value of Rem for the flow that is capable of sustaining the steady-state dynamo-process is achieved at $\ell = 0$.

The volume ponderomotive forces $[\vec{H} \times \mathrm{rot}\vec{H}]$, while perturbing the velocity field in compliance with the equation (2), bring about an increase in tangential strains that slow down the plate movement. In this way, the transformation of mechanical energy into electromagnetic is provided, determining, after all, the essence of the hydromagnetic dynamo effect.

3. Shear flow structure in planet liquid cores accounted for by tidal slow-down of the external solid shell

During the first stage of shear flow modeling, it is necessary to determine the velocity profile in the liquid core, rotating in inertia together with the innermost solid core, with a weak slowdown of the external shell (mantle), as caused by the impetus of tidal forces. The way to solution of this problem is in brief as follows. Firstly, the hydrodynamic problem is solved at the condition of a negligibly low influence of magnetic field on the flow.

The fluid motion equation is considered to be initial in such reference system that is associated with the external spherical shell, rotating with the angular velocity $\vec{\Omega} = \Omega\vec{e}_z$

$$\frac{\partial\vec{V}}{\partial t} - [\vec{V} \times \vec{\Gamma}] + 2[\vec{\Omega} \times \vec{V}] = -\mathrm{grad}\, W + \eta\Delta\vec{V}, \quad (\mathrm{div}\vec{V} = 0), \quad (24)$$

where $\vec{V}$ – the flow velocity, $\vec{\Gamma} = \mathrm{rot}\vec{V}$, W – the generalized potential.

The conditions of non-flow and stickiness on solid boundaries are considered to be assigned as commonly accepted in the viscous fluid hydrodynamics. Employment of the operation to (24) leads to the equation:

$$\frac{\partial\vec{\Gamma}}{\partial t} = \mathrm{rot}[\vec{V} \times \vec{\Gamma}] + 2\Omega\frac{\partial\vec{V}}{\partial z} + \eta\Delta\vec{\Gamma}. \quad (25)$$

The following linearized equations are obtained from (24) and (25) from the axially symmetric steady-state flow, while choosing such a system of units in which $\Omega = 1$, neglecting the squared terms and having in mind a low intensity of the differential rotation:

$$\eta\Delta\vec{V} - 2[\vec{e}_z \times \vec{V}] = \mathrm{grad}\, W, \quad (26)$$

$$\eta\Delta\vec{\Gamma} + 2\frac{\partial\vec{V}}{\partial z} = 0. \quad (27)$$

The velocity field that satisfies the condition of incompressibility $\mathrm{div}\vec{V} = 0$ in a cylindrical coordinate system can be represented in the following way:

$$\vec{V} = \mathrm{rot}(F\vec{e}_\varphi) + V_\varphi\vec{e}_\varphi = -\frac{\partial F}{\partial z}\vec{e}_\rho + V_\varphi\vec{e}_\varphi + \frac{1}{\rho}\frac{\partial}{\partial\rho}(\rho F)\vec{e}_z, \quad (28)$$

where $F = F(\rho, z)$, $V_\varphi = V_\varphi(\rho, z)$ – the sought functions. To determine them one can use just projections of the equations (26) and (27) on the azimuthal direction:

$$\eta\Delta_1 V_\varphi + 2\frac{\partial F}{\partial z} = 0,$$
$$\eta\Delta_1\Gamma_\varphi + 2\frac{\partial V_\varphi}{\partial z} = 0,$$

where $\Delta_1 = \frac{1}{\rho}\frac{\partial}{\partial\rho}\left(\rho\frac{\partial}{\partial\rho}\right) + \frac{\partial^2}{\partial z^2} - \frac{1}{\rho^2}$. Inasmuch as $\Gamma_\varphi = \mathrm{rot}_\varphi\vec{V} = -\Delta_1 F$, then for F and V_φ we have the following equation set in particular derivatives:

$$\begin{aligned} &\varepsilon\Delta_1 V_\varphi + \frac{\partial F}{\partial z} = 0, \\ &-\frac{\partial V_\varphi}{\partial z} + \varepsilon^2\Delta_1^2 F = 0 \end{aligned} \quad (29)$$

with the small parameter $\varepsilon = \sqrt{\eta/2}$ at differential operators of the second and fourth orders.

The derived set (29) is singularly perturbed. Quite naturally for this reason, it is deemed expedient for its solution to bring out boundary layers from the region of determination of the functions V_φ and F in order to gain capability of renormalizing the space scale in their vicinity, while in the remaining internal volume one could use the following simplified equations, acting on the assumption that $\varepsilon = 0$

$$\frac{\partial F}{\partial z} = 0, \qquad \frac{\partial V_\varphi}{\partial z} = 0,$$

from which it follows that in the internal volume $F = F(\rho)$, $V_\varphi = V_\varphi(\rho)$. There are 3 boundary layers in the considered flow: two running near the wall that are adjacent to the spheres $r = 1$ and $r = a$ and marked with the indices "e" and "i" respectively and also an internal boundary layer in the vicinity of the equatorial plane that is accounted for by the mirror symmetry of the velocity field. It is quite understood that the "boundary layer" and "internal volume" solutions must be reciprocally matched on some earlier unknown surfaces which are to be determined with the progression of the problem on the whole based on the conditions of the kinematic and dynamic compatibility.

In the spherical coordinates the equation set (29) takes on the following form:

$$\begin{aligned} &\varepsilon^2\Delta_1 V_\varphi + \frac{\partial F}{\partial r}\cos\theta - \frac{1}{r}\frac{\partial F}{\partial \theta}\sin\theta = 0, \\ &-\frac{\partial V_\varphi}{\partial r}\cos\theta + \frac{1}{r}\frac{\partial V_\varphi}{\partial \theta}\sin\theta + \epsilon^2\Delta_1^2 F = 0, \end{aligned} \tag{30}$$

where

$$\Delta_1 = \frac{1}{r^2}\frac{\partial}{\partial r}\left(r^2\frac{\partial}{\partial r}\right) + \frac{1}{r^2\sin\theta}\frac{\partial}{\partial\theta}\left(\sin\theta\frac{\partial}{\partial\theta}\right) - \frac{1}{r^2\sin^2\theta}. \tag{31}$$

While in the internal region we have $F = F(r\sin\theta)$, $V_\varphi = V_\varphi(r\sin\theta)$.

In the near-wall boundary layer, in the vicinity of each point of the boundary $r = 1$ (or $r = a$, where a – the internal core radius) we introduce local coordinates x and y at $\theta = \vartheta$, substituting r and τ according to the formulae:

$$r = 1 + \varepsilon x \quad (\text{or} \quad r = a + \varepsilon x), \quad \theta = \vartheta + \varepsilon y.$$

We now present the sought-after solution in the following way:

$$\begin{aligned} V_\varphi &= \varepsilon[v_0(\lambda,\vartheta) + \varepsilon y v_1(\lambda,\vartheta)], \\ F &= \varepsilon^2[f_0(\lambda,\vartheta) + \varepsilon y f_1(\lambda,\vartheta)], \end{aligned} \tag{32}$$

where $\lambda = c(\vartheta)x$, $c(\vartheta) = \frac{\sqrt{2}}{2}\sqrt{|\cos\theta|}$. Substituting it in the equation set (30) and providing the identity over y, in the first approximation over ε, we obtain a set of common differential equations of the 12-th order, with the coefficients being constant relative to λ:

$$\begin{aligned} &v_0'' + 2c(\vartheta)\mathrm{sgn}\left(\frac{\pi}{2} - \vartheta\right) f_0' = 0, \\ &-2v_0' + c(\vartheta)\mathrm{sgn}\left(\frac{\pi}{2} - \vartheta\right) f_0^{IV} = 0, \\ &v_1'' + 2c(\vartheta)\mathrm{sgn}\left(\frac{\pi}{2} - \vartheta\right) f_1' = \frac{\sin\vartheta}{c(\vartheta)} f_0', \\ &-2v_1' + c(\vartheta)\mathrm{sgn}\left(\frac{\pi}{2} - \vartheta\right) f_1^{IV} = -2\,\mathrm{tg}\,\vartheta v_0'. \end{aligned} \tag{33}$$

Here, the primes stand for differentiation over λ.

To obtain 12 constants of integration and parameter λ_0, which determines the position of the boundary layer borderline, one should know 13 boundary conditions. In particular, six conditions are assigned for the boundary layer adjacent to the outer sphere, expressing the requirements for non-flow and adhesion to the wall $r = 1$ that have the following form in the local coordinates (λ, y):

$$\begin{aligned} &v_0^{(e)}(0,\vartheta) = 0,\ f_0^{(e)}(0,\vartheta) = 0,\ f_0^{(e)'}(0,\vartheta) = 0, \\ &v_1^{(e)}(0,\vartheta) = 0,\ f_1^{(e)}(0,\vartheta) = 0,\ f_1^{(e)'}(0,\vartheta) = 0, \end{aligned} \tag{34}$$

with the remaining seven conditions –

$$\begin{aligned} &v_0^{(e)}(\lambda_0^{(e)},\vartheta) = \sin\theta|\cos\theta|^{1/2}, \\ &v_0^{(e)'}(\lambda_0^{(e)},\vartheta) = 0, \qquad f_0^{(e)'}(\lambda^{(e)},\vartheta) = 0, \\ &f_0^{(e)''}(\lambda_0^{(e)},\vartheta) = 0, \qquad v_1^{(e)}(\lambda_0^{(e)},\theta) = 0, \\ &f_1^{(e)}(\lambda_0^{(e)},\theta) = 0, \qquad f_1^{(e)'}(\lambda_0^{(e)},\vartheta) = 0 \end{aligned} \tag{35}$$

bearing the requirements for the kinematic and dynamic conjugation of the boundary layer solution with the volume one.

The boundary layer solution provides for the spectrum of eigen values $\lambda_n^{(e)} = -(n+1)\pi$ (n – the integer), from which only $\lambda_0^{(e)} = -\pi$ is physically realizable. Such eigen functions $v_0^{(e)}(\lambda,\vartheta)$, $f_0^{(e)}(\lambda,\vartheta)$, $v_1^e(\lambda,\vartheta)$, $f_1^{(e)}(\lambda,\vartheta)$ are constructed that correspond to this value of , the concrete expressions of which are given in [20], where the boundary layer problems are solved in a similar way on the internal (solid) core and in the vicinity of the equatorial plane, also observing the conditions of conjugation with flow in the internal volume.

An analysis of flow structure in the vicinity of the boundary of solid core, located in the region of almost uniform fluid rotation, indicated that it does not, practically, perturb the velocity field, and since its conduction is almost the same as the liquid core has, its influence on the magnetic field generation is not of any importance.

The intra-volume flow in the lowermost order over has the only azimuthal component $V_\varphi(r,\vartheta) = \varepsilon V(r,\vartheta)$, where

$$V(r,\vartheta) = r\sin\theta(1 - r^2\sin^2\theta)^{1/4}.$$

This is exactly the principal result of studies on the velocity field structure of a quasi-steady-state flow, appearing as a result of a relatively weak tidal slowdown of the external shell. The volume flow axial component is, according to (28) and (32), of the order ε^2, i.e. it is less intense by an order of magnitude that the azimuthal one. Regarding flows in the boundary layers, they have the same intensity as $V_\varphi(r,\vartheta)$ owing to the conjugation conditions, but being extremely thin, they cannot noticeably perturb the magnetic field. Although the hydrodynamic part of the problem is solved with an accuracy to ε^2 in all details, yet the studies on magnetic field generation call for understanding the azimuthal velocity profile, just given here, that depends drastically on the radius ρ and does not on z, i.e. having the nature of plane differential rotation.

4. Magnetic field generation by differentially rotating liquid conductive planet core

At the final stage of this study, it remains to be convinced that the said differential flow velocity profile in the liquid core really leads to the magnetic field generation. Here, the magnetic field inductance equation is initial

$$\frac{\partial \vec{H}}{\partial t} = \mathrm{rot}[\vec{V} \times \vec{H}] + \mu \Delta \vec{H}, \quad (\mathrm{div}\vec{H} = 0), \qquad (36)$$

where $\vec{V} = \vec{e}_\varphi r \sin\vartheta (1 - r^2 \sin^2\vartheta)^{1/4}$, μ – the magnetic viscosity, determined considering the intensity of differential rotation. As a boundary condition, the requirement for current non-flow through the boundary $r = 1$ of the external non-conductive shell is used

$$J^r = \mathrm{rot}_r \vec{H}\big|_{r=1} = 0. \qquad (37)$$

The solution is presented as the expansion

$$\vec{H}(r, \vartheta, \varphi, t) = \sum_\nu h_\nu \vec{H}_\nu(r, \vartheta) e^{i(m\varphi - \omega t)} \qquad (38)$$

($\nu = \{m, n, l\}$ – the multi-index; m, n, l – the azimuthal, poloidal and radial wave numbers over the eigen vector-functions $\vec{H}_\nu(r, \vartheta)$ of the Laplace operator that are solutions of the Helmholtz vector equations

$$(\Delta + k_\nu^2)\vec{H}_\nu e^{im\varphi} = 0. \qquad (39)$$

Instead of $\vec{H}_\nu(r, \vartheta)$ it is more convenient to use the appropriate current density harmonics $\vec{J}_\nu = \mathrm{rot}\vec{H}_\nu$, which in their turn admit the representation of $\vec{J}_\nu = \mathrm{rot}(\Gamma_\nu \vec{e}_z)$ through spherical harmonics Γ_ν of the z-component of the Hertz vector, satisfying the Helmholtz scalar equation

$$\Delta \Gamma_\nu + k_\nu^2 \Gamma_\nu = 0,$$

with the boundary condition (37), in the case of satisfaction of the Dirichlet condition $\Gamma_\nu\big|_{r=1} = 0$, being satisfied for $\vec{J}_\nu$ automatically, since

$$J_v^r = \mathrm{rot}_r[\Gamma_\nu(\vec{e}_r \cos\vartheta - \vec{e}_\vartheta \sin\vartheta)] = -\frac{im}{r}\Gamma_\nu.$$

In the basis $\vec{J}_\nu$ the equation (13) assumes the following form:

$$\sum_\nu \Big\{ i\Big\langle \vec{J}_\nu \cdot \Big[\vec{V} \times \mathrm{rot}\vec{J}_\nu\Big]\Big\rangle - \Big(\omega + i\mu k_\nu^2\Big)\Big\langle \vec{J}_{\nu'} \cdot \vec{J}_\nu \Big\rangle \Big\} g^\nu = 0,$$
$$(\nu' = 1, 2, 3, ...), \qquad (40)$$

where $g^\nu = k_\nu^{-2} h^\nu$, while the symbol $\langle\cdot\rangle$ stands for the scalar product of two arbitrary vector functions $\vec{f}$ and $\vec{g}$:

$$\Big\langle \vec{f}(r, \vartheta) \cdot \vec{g}(r, \vartheta) \Big\rangle = \int_0^1 \int_0^\pi \Big(\vec{f}^* \cdot \vec{g}\Big) r^2 \sin\vartheta dr d\vartheta$$

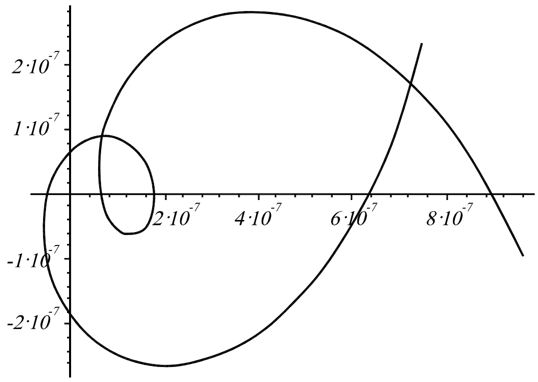

Fig. 11. Instability: $\mu = 0.0025$, $\omega = 0.75..1.08$.

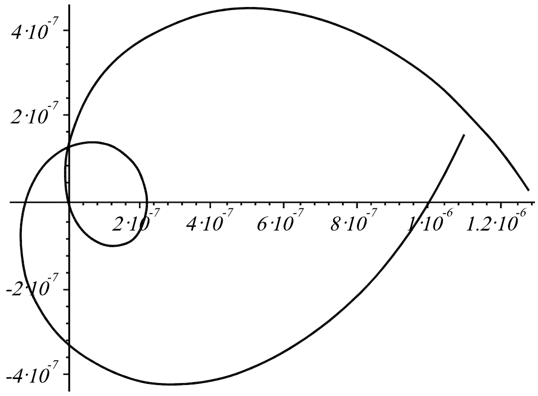

Fig. 12. Neutral: $\mu = 0.00260964765$, $\omega = 0.75..1.08$.

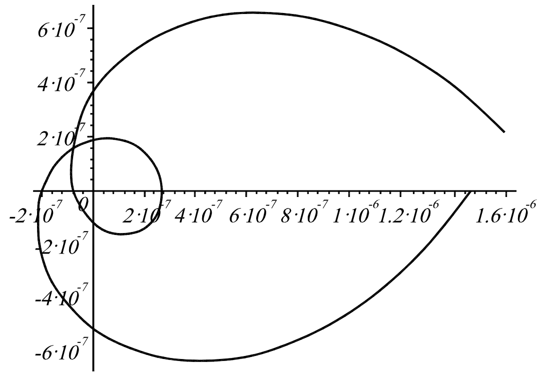

Fig. 13. Neutral: $\mu = 0.0027$, $\omega = 0.75..1.08$.

where $*$ – the complex conjugation.

By designating

$$\Big\langle \vec{J}_{\nu'} \cdot \vec{J}_\nu \Big\rangle = m_{v'v}, \qquad i\Big\langle \vec{J}_{\nu'} \cdot \Big[\vec{V} \times \mathrm{rot}\vec{J}_\nu\Big]\Big\rangle = N_{\nu'\nu}, \qquad (41)$$

we shall obtain the infinite equation set

$$\sum_\nu \left[N_{\nu'\nu} + (\omega + i\mu k_\nu^2) m_{\nu'\nu}\right] g^\nu = 0,$$
$$(\nu' = 1, 2, 3, ...). \qquad (42)$$

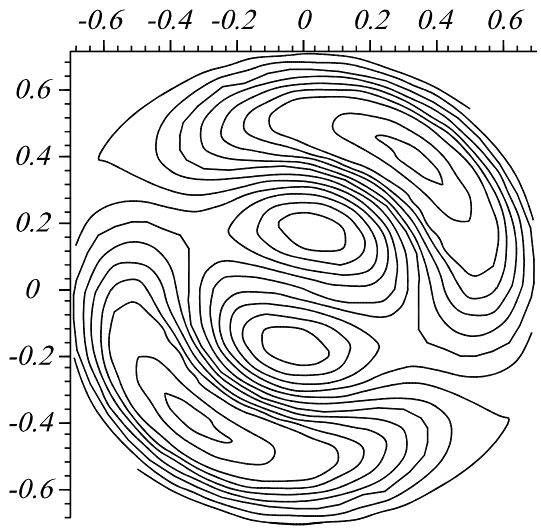

Fig. 14. J^r, $Z = 0.75$

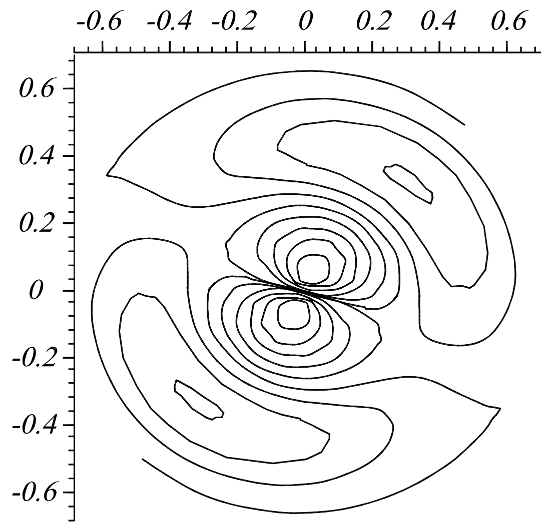

Fig. 15. J^θ, $Z = 0.75$

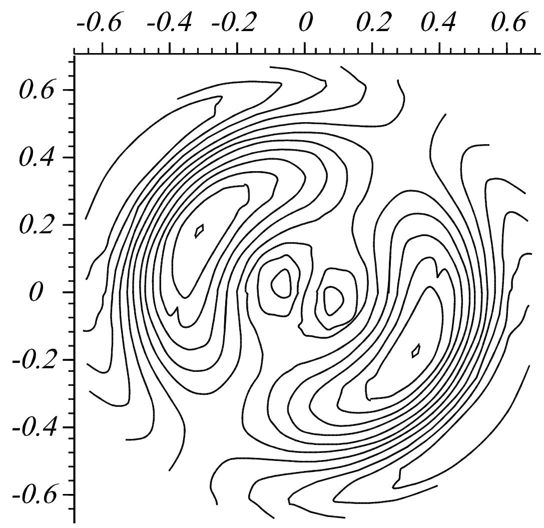

Fig. 16. J^φ, $Z = 0.75$

For its non-trivial solution to exist one should require that

$$\det\left|N_{\nu'\nu} - (\omega + i\mu k_\nu^2) m_{\nu'\nu}\right| = 0. \tag{43}$$

Having obtained the roots ω_σ ($\sigma = 1, 2, 3, \dots$) of the characteristic equation (43) and appropriate modal columns g_σ^ν of the equation (42), we obtain the proper numbers and eigen vectors of the above formulated boundary problem.

At the condition that μ should be smaller than a certain critical value $\mu_{\rm cr}$, for a certain sub-set of proper numbers ω_σ there will be $\operatorname{Im}\omega_\sigma > 0$. This sub-set corresponds to current and magnetic field perturbations exponentially growing vs. time. At $\mu = \mu_{\rm cr}$ all the inductance equation solutions decay, but one, which is neutrally stable. Then in the case of the appropriate $\sigma = \sigma_0$, at which $\operatorname{Im}\omega_{\sigma_0} = 0$, the value $\omega_0 = \operatorname{Re}\omega_{\sigma_0} \neq 0$ characterizes the generated magnetic field drift relative to the reference frame associated with the solid shell.

Numeric solution of the problem for each fixed presupposes the limitation by a certain number N of the dimensionality of the considered space of harmonics ordered over k_ν. It turned out that for the azimuthal wave number $m = 1$ and a series of odd poloidal wave numbers n at $N = 12$ $\mu_{\rm cr} = 0.002609647965$, while $\omega_0(N) = 0.985685478805$. Determination of the number $N = N^*$ which should be sufficient for a necessary approximation accuracy must be made, viewing the fact of stabilization of the monotonously growing $\mu_{\rm cr}(N)$, which strives to attain a certain limit μ^*. For the problem of planetary dynamo the determination $\mu^* = \operatorname{Re}_m^{-1}$ is of fundamental importance.

Having in mind the fact that the left-hand part of the characteristic equation (43) for $N = 12$ is a polynomial of the 12-th order relative to ω, with the complex coefficients depending on the parameter μ, the direct derivation of all the roots ω_σ (12) seems practically unsubstantiated. Instead it is expedient to employ the principle of argument for root position localization determination on the complex plane relative to the real axis, separating the set of all roots into sub-sets of those stable and unstable. It is just sufficient to build a locus of the polynomial at each fixed μ as a function of ω, varying along the real axis from $-\infty$ to $+\infty$. Having determined the number of revolutions of this locus round the beginning of the coordinates, one can pass judgement about the presence of unstable roots and their number. In particular, for $N = 12$, if all solutions are the decaying ones, the locus makes $N/2 = 6$ revolutions clockwise. If one root is neutrally stable, then the locus makes 5 full revolutions, passing once through the beginning of the coordinates. And, finally, if it does not pass through the beginning of the coordinates and makes less than 6 revolutions clockwise, then the set has unstable solutions. These cases are illustrated for a fragment of this locus near the beginning of the coordinates in fig. 11–13. According to the values that have been found and one can locate the appropriate modal column and a particular solution for the current density and magnetic field.

Results of the calculations in the form of level curves for radial, poloidal and azimuthal current density are shown in fig. 4–6. In these figures, very noticeable is a spiral curling of the current density distribution, caused by the differential rotation.

5. Conclusions

In order to study the tidal mechanism of planetary magnetic field generation, this paper investigates the flow structure in the plane and spherical layers of a weakly viscous fluid that is limited by non-conducting shells moving in the opposite directions with different velocities. It is established for a fact that at the condition of a strong influence of Coriolis accelerations in the spherical geometry, besides the sub-surface boundary layers there also appears an internal boundary layer with the flow radial direction in the vicinity of the equatorial plane at the junction of weak opposite flows of the axial directivity. It is also clear that in the internal volume the rotary fluid motion has an angular velocity that is substantially dependent on the radius, i.e. of quite non-solid-state nature, as had been assumed earlier. It is exactly these properties of the velocity field structure in the core that allowed one to prove a possibility of magnetic field self-excitation at a relatively high ($10^2 \div 10^3$) Reynolds number. To date epures of magnetic fields and currents have been constructed on the linear level of modeling in consideration of the condition of non-conduction of limiting surfaces. The obtained results have some promise of doing further research into the tidal mechanism of the hydromagnetic planetary dynamo.

References

[1] Moffat G. Manetic field excitation in the conducting medium – Moscow: Mir Publishers. – 1980. – 340 p.

[2] Hollerbach R., Jones C.A. A geodynamo model incorporating a finitely conducting inner core. Physics of the Earth and Planetary Interiors // – 1993. – V. 75. – P. 317–327.

[3] Busse F.H. Magnetohydrodynamics of the Earth's dynamo // Ann. Rev. Fluid Mech. – 1978. – V. 10. – P. 435–462.

[4] Cowling T.G. The magnetic field of sunspots // Month. Not.Roy. Astron. Soc. – 1943. – V. 94. – P. 39–48.

[5] Backus G. Kinematics of geomagnetic secular variations in a perfectly conducting core. // London: Philos.Trans. R. Soc. — 1968. — Ser. A. 263. – P. 239–266.

[6] Herzenberg A. Geomagnetic dynamos // London: Philos.Trans. R. Soc. – 1958. – Ser. A.250. – P. 543–585.

[7] Larmor J. How could a rotating body such as the Sun become a magnet? // Rep. Brit. Assoc. Adv. Sci. – 1919. – P. 159–160.

[8] Roberts P.H. Dynamo theory. // In Mathematical Problems in the Geophysical Sciences. Ed. W.A. Reed. – Providence, R.I.: Am. Math. Soc. – 1971. – P. 129–206.

[9] Glatzmaier G.A., Roberts P.H. A three-dimensional self-consistent computer simulation of a geomagnetic field reversal // Nature. – 1995. – V. 377. – P. 203–209.

[10] Braginsky S.I. Nearly axially symmetric model of the hydromagnetic dynamo of the Earth. I // Geomag. Air Nav. – 1975. – V. 15. – P. 149-156.

[11] Parker E.N. Hydromagnetic dynamo models // Astrophys. J. – 1955. – V. 122. – P. 293–314.

[12] Dolginov S.S. Magnetism of planets. Moscow, Znaniye Publishers, 1974, 64 p.

[13] Proudman I. The almost-rigid rotation of viscous fluid between concentric spheres. // J. Fluid Mech. – 1956. – V. 1. – P. 505–516.

[14] Elsasser W.M. Induction effects in terrestrial magnetism // I. Theory, Phys. Rev. – 1946. – V. 69. – P. 106–116.

[15] Cowling T. Magnetic hydrodynamics – M.: Atomizdat. – 1978. – 144 p.

[16] Crechetov V.V. Tidal forces and magnetic field generation of planets // Kosmicheskiye Issledovaniya. – 1999. – V 37, N 4. – P. 392–396.

[17] Stacey, F. Physics of the Earth – M.: Mir. – 1972. – 343 p.

[18] Olver F. Introduction into asymptotic methods and special function – M.: Nauka. – 1978. – 376 p.

[19] Fock, V.A. Airy function tables. – M.: Dept.NII-108. – 1946. 56 p.

[20] Samoilenko Yu.I., Loginov A.A., Tkachenko V.A.. Geomagnetic field generation modeling // Vestnik of Kherson State Technical Univ. – 2001. – N 3 (12). – P. 235–244.